ON TRACKING-DRIVEN ROAD MAP EXTRACTION FROM GMTI RADAR DATA

W. Koch, M. Ulmke

FGAN-FKIE, D 53343 Wachtberg, Germany – (w.koch,ulmke)@fgan.de

KEY WORDS: road extraction, ground moving target indication radar (GMTI), target tracking, road moving targets, retrodiction

ABSTRACT

For analyzing dynamic scenarios characterized by many ground moving vehicles, airborne GMTI radar is a well-suited sensor due to its wide-area, all-weather, day/night, and real time capabilities (GMTI: Ground Moving Target Indicator). The generation of GMTI tracks from these data is the backbone for producing a "recognized ground picture" as well as for analyzing traffic flows. In this paper we dicuss the benefits of GMTI tracking in view of extracting road map information from GMTI data. The resulting tracking-generated road maps are highly up-to-date and fairly precise. Moreover, their accuracy is quantitatively described. The proposed approach to road map extraction is essentially based on a temporal integration of the received sensor data and by this differs in nature from methods based on pattern recognition in a single image.
The underlying idea is rather simple: By definition, the track of a road moving target provides an approximation of the underlying road. As GMTI tracking is a highly challenging task, the quality of GMTI tracks, however, is often insufficient for road map production due to false returns, missing detections, Doppler blindness, fading phenomena, and other reasons. In this context, retrodiction techniques can provide significant improvements. Being a generalization of standard smoothing techniques to multiple hypothesis tracking (or, more generally speaking, Gaussian sum or particle filtering), retrodiction provides fairly precise estimates of the target kinematics at past time instants by exploiting the sensor information available up to the present time. From 'retrodicted tracks' the road position and related tangential vectors to the road can easily be derived. For calculating additional supporting vectors 'continuous time retrodiction' is proposed. We indicate how the generated road map information is exploited in the tracking loop resulting in even more precise tracks. A procedure for iteratively producing high-precision road maps due to changing sensor-to-target geometries is sketched.
The proposed approach is illustrated be a simulated example providing hints to the achievable road map accuracies. An important application is the mitigation of sensor registration errors by matching the produced sensor individual road maps with each other and with geo-referenced road maps available in a topographical data base.

1 INTRODUCTION

The analysis of dynamic scenarios characterized by many ground moving vehicles is an important task with numerous military and civil applications. For producing appropriate surveillance data to be exploited, airborne GMTI radar is a well-suited sensor due to its wide-area, all-weather, day/night, and real time capabilities (GMTI: Ground Moving Target Indicator).

The processing of GMTI measurements of kinematical target parameters (range, azimuth, range-rate) results in the production of GMTI tracks, which represent the currently available knowledge on the kinematical properties of ground moving objects along with related measures of accuracy and the corresponding history (1, 2, 4). GMTI tracks are thus prerequisites for producing a "recognized ground picture" as well as for analyzing traffic flows.

In most applications the majority of ground vehicles is moving on road networks whose topographical coordinates might be known at least up to a certain accuracy. Such road maps provide valuable context information which can be used for improving the quality of GMTI tracking (5, 6, 7, 8, 9). This does not only affect the achievable track accuracy but also the weighting factors for association hypotheses in MHT techniques (Multiple Hypothesis Tracking) or, more generally, the problem of track continuity and track separation.

Seen from a different perspective, however, ground vehicles moving on road networks being observed by wide-area sensors, such as GMTI radar, produce large data streams that can also be used for road map extraction: After a suitable post-processing described in this paper, the GMTI tracks of road targets simply define the corresponding road segments currently being used by the ground moving targets.

Tracking-driven road extraction can be beneficial in situations or scenarios where reliable road maps are not available at all, where the maps provided by geographical information systems are not up-to-date, or where the accuracy of the road maps is insufficient. In addition, there exist fields of applications, in which roads or road-like 'lines of communication' exist only temporarily or may change with time. This can be the case in deserts or in times of a conflict. As practical evidence shows, even in typical off-road scenarios the existence of structures similar to roads quickly evolve, as a 'second' vehicle usually moves in the tracks of its precursor. This is especially true in a not sufficiently explored or a dangerous environment (e.g. in a mine field).

In the sensor's own coordinate system, the achievable accuracy of road maps generated by road target tracking depends on the measurement accuracies of the GMTI sensors, the current sensor-to-target geometry, the scan rate, and the dynamic properties of the ground targets, i.e. on the accuracy of the produced GMTI tracks. As usually many targets use the same road segments, a significant gain results from fusing several "road tracks". In addition the underlying sensor-to-target geometry is continuously changing with time as GMTI radar is essentially an airborne, i.e. a moving, sensor system. For this reason the fusion of "road tracks" produced at different instants of time is expected to improve the achievable accuracy of track-generated road maps even more, finally leading to high-precision road maps.

Sensor registration or misalignment errors usually cause serious problems in sensor data fusion. In other words, in a given sensor data fusion application it cannot always be taken for granted that the data originating from various distributed sensors can be transformed into a common coordinate system. For mitigating the corresponding bias errors, the tracking-driven generation of

accurate road maps with reference to the individual sensor coordinate system can well be used. Precisely extracted road maps with reference to the coordinate system of the individual sensors can easily be matched with each other by using particular road map features such as characteristic curves or crossings. By this a compensation of relative bias errors can easily be achieved. A contribution to remove also *absolute* bias errors is obtained by matching tracking-generated road maps with geo-referenced maps stored in a topographical data base.

2 ELEMENTS OF GMTI TRACKING

In a BAYESian view, a tracking algorithm is an iterative updating scheme for conditional probability density functions (pdf) $p(\mathbf{x}_k|\mathcal{Z}^k, \textit{'background'})$ that statistically describe the kinematical state vector $\mathbf{x}_k$ of a target at discrete revisit times t_k given both, the accumulated GMTI sensor data $\mathcal{Z}^k = \{Z_l\}_{l=1}^k$ up to time t_k and all available background information. Z_l denote the data of the radar scan at time t_l relevant for the target currently under track.

Each update of $p(\mathbf{x}_k|\mathcal{Z}^k)$ consists of a prediction step that exploits the target dynamics model and road map information if it is available. The prediction is followed by a subsequent filtering step, where the newly received sensor data are processed by making use of the underlying sensor model. Retrodiction (or smoothing) is a backwards directed iteration for calculating the conditional probabilities $p(\mathbf{x}_l|\mathcal{Z}^k)$, $l < k$, that describe the past target states $\mathbf{x}_l$ given all sensor data up to the present time t_k. This process is illustrated by the following scheme:

$$\text{prediction:} \quad p(\mathbf{x}_{k-1}|\mathcal{Z}^{k-1}) \xrightarrow[\text{road maps}]{\text{dynamics}} p(\mathbf{x}_k|\mathcal{Z}^{k-1}) \tag{1}$$

$$\text{filtering:} \quad p(\mathbf{x}_k|\mathcal{Z}^{k-1}) \xrightarrow[\text{new data } Z_k]{\text{sensor model}} p(\mathbf{x}_k|\mathcal{Z}^k) \tag{2}$$

$$\text{retrodiction:} \quad p(\mathbf{x}_l|\mathcal{Z}^k) \xleftarrow[\text{model}]{\text{dynamics}} p(\mathbf{x}_{l+1}|\mathcal{Z}^k), \; l < k. \tag{3}$$

By assuming suitable cost criteria (e.g. MMSE (10)), the probability density functions $p(\mathbf{x}_l|\mathcal{Z}^k)$ provide state estimates $\mathbf{x}_{l|k}$ with related covariance matrices $\mathbf{P}_{l|k}$ ($l > k$: prediction, $l = k$: filtering, $l < k$: retrodiction), which can be written as:

$$\mathbf{x}_{l|k} = \begin{pmatrix} \mathbf{r}_{l|k} \\ \dot{\mathbf{r}}_{l|k} \end{pmatrix}, \quad \mathbf{P}_{l|k} = \begin{pmatrix} \mathbf{R}_{l|k} & \mathbf{Q}_{l|k} \\ \mathbf{Q}_{l|k} & \dot{\mathbf{R}}_{l|k} \end{pmatrix}. \tag{4}$$

The subscripts denote that the quantities are related to t_l based on all measurements up to and including t_k. As in any practical application ambiguity due to the uncertain origin of the sensor data or particular sensor models must be taken into account, the densities in general prove to be finite mixtures (11, 12, 13), i.e. weighted sums of individual probability densities.

Let the kinematical state vector of a ground moving target at time t_k be given by its current position $\mathbf{r}_k = (x_{k;1}, x_{k;2}, x_{k;3})^\top$ and velocity $\dot{\mathbf{r}}_k$ in earth-fixed Cartesian coordinates:

$$\mathbf{x}_k = \left(\mathbf{r}_k^\top, \dot{\mathbf{r}}_k^\top\right)^\top = (x_{k;1}, \ldots, x_{k;6})^\top. \tag{5}$$

Due to the small agility of ground targets, acceleration components are omitted. In a flat-earth approximation, we in particular have: $x^g_{k;3} = x^g_{k;6} = 0$. In the ground coordinate system the target dynamics is modeled by a linear system equation with additive white Gaussian noise (10, 11). With a scalar plant noise variance $\Sigma^2_{k|k-1}$ given by $\Sigma_{k|k-1} = v_t\left(1 - \mathrm{e}^{-2(t_k - t_{k-1})/\theta_t}\right)^{1/2}$ (parameters v_t and θ_t discussed below), 3D diagonal matrices $\mathbf{J} = \mathrm{diag}[1,1,0]$, $\mathbf{O} = \mathrm{diag}[0,0,0]$, and a noise component $\mathbf{v}_k \sim N(0, \mathbf{J})$, let us consider the following realization (14):

$$\mathbf{x}_k = \mathbf{F}_{k|k-1}\mathbf{x}_{k-1} + \mathbf{G}_{k|k-1}\mathbf{v}_k \tag{6}$$

with matrices $\mathbf{F}_{k|k-1}$ and $\mathbf{G}_{k|k-1}$ given by:

$$\mathbf{F}_{k|k-1} = \begin{pmatrix} \mathbf{J} & (t_k - t_{k-1})\mathbf{J} \\ \mathbf{O} & \mathrm{e}^{-(t_k - t_{k-1})/\theta_t}\mathbf{J} \end{pmatrix} \tag{7}$$

$$\mathbf{G}_{k|k-1} = \Sigma_{k|k-1}\begin{pmatrix} \mathbf{O} \\ \mathbf{J} \end{pmatrix}. \tag{8}$$

According to this dynamics model, the velocity $\dot{\mathbf{r}}_k$ is described by an ergodic MARKOV process with $\mathbb{E}[\dot{\mathbf{r}}_k] = 0$. The corresponding autocorrelation function is given by $\mathbb{E}[\dot{\mathbf{r}}_k \dot{\mathbf{r}}_l{}^\top] = v_t^2 \, \exp[-|t_k - t_l|/\theta_t] \, \mathbf{J}$, $l \le k$. This expression gives a clear meaning to the modeling parameters v_t (*limiting speed*) and θ_t (*maneuver correlation time*) in the plant noise variance $\Sigma_{k|k-1}$. In contrast to the dynamics model used in (1), the model naturally introduces a 'speed limit' v_t, while θ_t may characterize different target types.

3 A MODELING OF ROADS

A given road through a real road network is mathematically described by a continuous 3D curve $\mathcal{R}^*$ in Cartesian ground coordinates. For the sake of simplicity the effect of crossroads is not considered here. See (8) for a more detailed discussion. Let $\mathcal{R}^*$ be parameterized by the corresponding arc length l. The exploitation of digitized road maps provides the data base for a piecewise linear approximation of the road curve $\mathcal{R}^* : l \mapsto \mathcal{R}^*(l)$ by a polygonal curve $\mathcal{R}$. Let us furthermore assume that the curve $\mathcal{R}$ is characterized by n_r node vectors

$$\mathbf{s}_m = \mathcal{R}^*(l_m), \quad m = 1, \ldots, n_r. \tag{9}$$

From the these quantities $n_r - 1$ normalized tangential vectors

$$\mathbf{t}_m = \frac{(\mathbf{s}_{m+1} - \mathbf{s}_m)}{||\mathbf{s}_{m+1} - \mathbf{s}_m||}, \quad m = 1, \ldots, n_r - 1 \tag{10}$$

can be derived. The EUCLIDian distance $||\mathbf{s}_{m+1} - \mathbf{s}_m||$ between two adjacent node vectors, however, is usually not identical with the distance $\lambda_m = l_{m+1} - l_m$ actually covered by a vehicle when it moves from $\mathbf{s}_m$ to $\mathbf{s}_{m+1}$ along the road. Besides the vectors $\mathbf{s}_m$ the scalar quantities $\lambda_m \ge |\mathbf{s}_{m+1} - \mathbf{s}_m|$ should therefore enter into the road model to make it more realistic. The differences $\lambda_m - ||\mathbf{s}_{m+1} - \mathbf{s}_m||$ can evidently serve as a quantitative measure of the discretization errors we have to deal with. Using the characteristic functions defined by

$$\chi_m(l) = \begin{cases} 1 & \text{for } l \in [l_m, l_{m+1}) \\ 0 & \text{else} \end{cases}, \; m = 1, \ldots, n_r - 1, \tag{11}$$

we obtain a mathematically simple description of the polygon curve $\mathcal{R}$, by which the road $\mathcal{R}^*$ is approximated:

$$\mathcal{R} : l \in [l_1, l_{n_r}) \mapsto \mathcal{R}(l) = \sum_{m=1}^{n_r - 1} \left[\mathbf{s}_m + (l - l_m)\mathbf{t}_m\right] \chi_m(l)$$
$$\text{with:} \quad \mathcal{R}^*(l_m) = \mathcal{R}(l_m) = \mathbf{s}_m, \quad m = 1, \ldots, n_r. \tag{12}$$

The accuracy by which the road is represented by the node vectors $\mathbf{s}_m$ can be described by a covariance matrix $\mathbf{R}_m$ characteristic of each node m. Typically these quantities, which are to

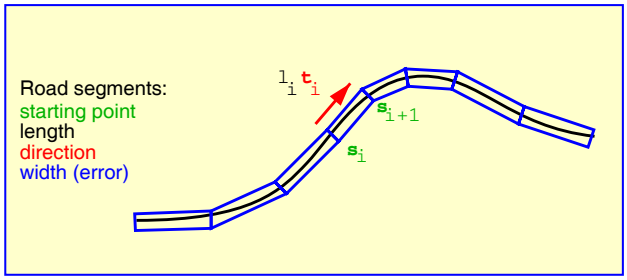

Figure 1: Representation of a road.

be used in road map assisted tracking, are not easily available as part of a geographical information data base. In case of tracking-generated road map, reliable estimates for these quantities do exist, as will become clear below. In summary a road segment is simply described by the pair $\mathcal{R}^* = \{\mathbf{s}_m, \mathbf{R}_m\}_{m=1}^{n_r}$ (eventually complemented by the numbers λ_m). See Figure 1 for illustration.

4 CONTINUOUS TIME RETRODICTION

According to the introductory remarks, the track of a road moving vehicle, i.e. the collection of expectations and covariance matrices $\{\mathbf{r}_{l|k}, \mathbf{R}_{l|k}\}_{l=1}^{k}$ provides by itself a first approximation of the road used by the vehicle. Due to low sensor update rates, missing detections, or fading phenomena, Doppler blindness etc., however, the accuracy and sample density of such track generated road maps may be insufficient.

In applications we therefore wish to produce a suitable interpolation between adjacent 'node vectors' and the related 'mapping error' covariance matrices. This interpolation should take full advantage of the available knowledge of the targets' kinematical state vector and the related track accuracy as well as of background information on the vehicle's behavior, i.e. the target dynamics model.

Given two adjacent nodes vectors $\mathbf{r}_{l-1|k}$, $\mathbf{r}_{l|k}$ with their related accuracies $\mathbf{R}_{l-1|k}$, $\mathbf{R}_{l|k}$, we at first have to decide whether it is reasonable to create an additional node at all. Obviously another node is necessary if there are curves or turns to be expected. Vice versa, for a more or less rectilinear road segment only very few nodes are required.

An intuitively clear indication for the existence of a winding road is given by comparing the direction of the velocity vector estimates $\dot{\mathbf{r}}_{l-1|k}$, $\dot{\mathbf{r}}_{l|k}$ at subsequent instants of time t_{l-1} and t_l, which by definition are proportional to estimates of the tangential vectors to the road at the locations $\mathbf{r}_{l-1|k}$ and $\mathbf{r}_{l|k}$. The decision also depends on the quality of these velocity estimates.

To introduce an additional node vector, let us denote by $\varphi_{l|k}$ the angle between the velocity estimate $\dot{\mathbf{r}}_{l|k}$ and one of the axes of the coordinate system. The corresponding angle for the actual velocity vector is a random variable approximately normal distributed with a variance given by $\Phi_{l|k}$. Let $\psi_{l|k}$ the corresponding angle of the difference vector $\mathbf{r}_{l+1|k} - \mathbf{r}_{l|k}$. An intuitively plausible decision criterion whether an additional node is to be introduced is thus given by:

$$(\varphi_{l|k} - \psi_{l|k})^2 / \Phi_{l|k} > \kappa^2. \tag{13}$$

If the inaccuracy of the heading estimates is large, subsequent headings are allowed to differ more than in case of more precise estimates. It seems to be reasonable to choose the decision parameter around One. Evidently, the estimate of the complete

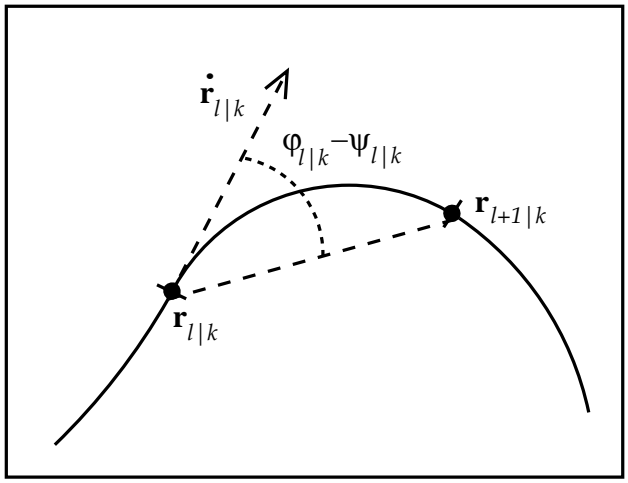

Figure 2: Adding a new node vector.

kinematical state vector enters into this criterion. See Figure 2 for a characteristic example and an intuitive interpretation of this criterion.

Given an additional node is to be introduced, let us consider the probability density $p(\mathbf{x}_{l-\theta}|\mathcal{Z}^k)$ with $0 < \theta < 1$, typically $\theta = \frac{1}{2}$ if $t_l = l\Delta t$. This density expresses the available knowledge about the kinematical target state at an intermediate instant of time $t_{l-1} < t_{l-\theta} < t_l$. From this density an intermediate node vector of the road and a tangential vector can be derived. By considering several $\theta_1, \theta_2, \ldots$ an indication of the arc length λ of the road between the positions $\mathbf{r}_{l-1}$ and $\mathbf{r}_l$ can be obtained.

Standard probability reasoning yields:

$$p(\mathbf{x}_{l-\theta}|\mathcal{Z}^k) = \int d\mathbf{x}_l \, p(\mathbf{x}_{l-\theta}|\mathbf{x}_l, \mathcal{Z}^k) \, p(\mathbf{x}_l|\mathcal{Z}^k). \tag{14}$$

In this expression the pdf $p(\mathbf{x}_l|\mathcal{Z}^k)$ is already known and in many cases at least approximately given by:

$$p(\mathbf{x}_l|\mathcal{Z}^k) = \mathcal{N}(\mathbf{x}_l;\, \mathbf{x}_{l|k},\, \mathbf{P}_{l|k}), \tag{15}$$

where $\mathbf{x}_{l|k}$ and $\mathbf{P}_{l|k}$ denote the expectation vector and the covariance matrix of a GAUSSian pdf. For the remaining factor in the previous integrand we obtain according to BAYES' rule:

$$p(\mathbf{x}_{l-\theta}|\mathbf{x}_l, \mathcal{Z}^k) = p(\mathbf{x}_{l-\theta}|\mathbf{x}_l, \mathcal{Z}^{l-1}) \tag{16}$$

$$= \frac{p(\mathbf{x}_l|\mathbf{x}_{l-\theta}) \, p(\mathbf{x}_{l-\theta}|\mathcal{Z}^{l-1})}{\int d\mathbf{x}_{l-\theta} \, p(\mathbf{x}_l|\mathbf{x}_{l-\theta}) \, p(\mathbf{x}_{l-\theta}|\mathcal{Z}^{l-1})}. \tag{17}$$

According to Equation 1,the probability density $p(\mathbf{x}_{l-\theta}|\mathcal{Z}^{l-1}) = \mathcal{N}(\mathbf{x}_{l-\theta};\, \mathbf{x}_{l-\theta|l-1},\, \mathbf{P}_{l-\theta|l-1})$ describes the knowledge available after data processing at time t_{l-1} and is also available. The transition density $p(\mathbf{x}_l|\mathbf{x}_{l-\theta})$ directly results from the target dynamics model (Equation 6) and is given by a GAUSSian as well:

$$p(\mathbf{x}_l|\mathbf{x}_{l-\theta}) = \mathcal{N}(\mathbf{x}_l;\, \mathbf{F}_{l|l-\theta}\mathbf{x}_{l-\theta},\, \mathbf{D}_{l|l-\theta}) \tag{18}$$

with $\mathbf{D}_{l|l-\theta} = \mathbf{G}_{l|l-\theta}\mathbf{G}_{l|l-\theta}^{\top}$. Algebraic reasoning finally yields:

$$p(\mathbf{x}_{l-\theta}|\mathbf{x}_l, \mathcal{Z}^k) = \mathcal{N}(\mathbf{x}_{l-\theta};\, \mathbf{x},\, \mathbf{P}) \tag{19}$$

$$\mathbf{x} = \mathbf{x}_{l-\theta|l-1} + \mathbf{W}_{l|l-\theta}(\mathbf{x}_l - \mathbf{F}_{l|l-\theta}\mathbf{x}_{l-\theta|l-1}) \tag{20}$$

$$\mathbf{P} = \mathbf{P}_{l-\theta|l-1} - \mathbf{W}_{l|l-\theta}\mathbf{P}_{l|l-1}\mathbf{W}_{l|l-\theta}^{\top} \tag{21}$$

$$\mathbf{W}_{l|l-\theta} = \mathbf{P}_{l-\theta|l-1}\mathbf{F}_{l|l-\theta}^{\top}\mathbf{P}_{l|l-1}^{-1}. \tag{22}$$

Insertion into Equation 14 leads to a modified version of the well-known Rauch-Tung-Striebel formulae (11):

$$p(\mathbf{x}_{l-\theta}|\mathcal{Z}^k) = \mathcal{N}(\mathbf{x}_{l-\theta};\, \mathbf{x}_{l-\theta|k},\, \mathbf{P}_{l-\theta|k}) \tag{23}$$

$$\mathbf{x}_{l-\theta|k} = \mathbf{x}_{l-\theta|l-1} + \mathbf{W}_{l|l-\theta}(\mathbf{x}_{l|k} - \mathbf{x}_{l|l-1}) \tag{24}$$

$$\mathbf{P}_{l-\theta|k} = \mathbf{P}_{l-\theta|l-1} + \mathbf{W}_{l|l-\theta}(\mathbf{P}_{l|k} - \mathbf{P}_{l|l-1})\mathbf{W}_{l|l-\theta}^{\top} \tag{25}$$

$$\mathbf{x}_{l|l-1} = \mathbf{F}_{l|l-1}\mathbf{x}_{l-1|l-1} \tag{26}$$

$$\mathbf{P}_{l|l-1} = \mathbf{F}_{l|l-1}\mathbf{P}_{l-1|l-1}\mathbf{F}_{l|l-1}^{\top} + \mathbf{D}_{l|l-1}. \tag{27}$$

5 ON ROAD MAP ASSISTED TRACKING

A first tracking-generated road map can be used for improving the track quality for a second vehicle moving on the same road. The resulting 'road map assisted' track in return will provide a better estimate of the underlying road. In this section we briefly sketch how road map information can be incorporated into the tracking process. For details see (3, 8).

In case of road moving targets it seems reasonable to describe the kinematical state vector $\mathbf{x}_k^r$ of road targets at time t_k by its position on the road l_k (i.e. the arc length of the curve) and its scalar speed $\dot{l}_k$: $\mathbf{x}_k^r = (l_k, \dot{l}_k)^{\top}$. The model for describing the dynamical behavior of road targets is therefore a 2D version of equation 6. By making use of the related transition density $p(\mathbf{x}_k^r|\mathbf{x}_{k-1}^r)$ the predicted density in road coordinates is given by

$$p(\mathbf{x}_k^r|\mathcal{Z}^{k-1}) = \int d\mathbf{x}_{k-1}^r\, p(\mathbf{x}_k^r|\mathbf{x}_{k-1}^r)\, p(\mathbf{x}_{k-1}^r|\mathcal{Z}^{k-1}). \tag{28}$$

The BAYESian formalism previously discussed can directly be applied to road targets, if it is possible to find a transformation operator $\mathcal{T}_{g\leftarrow r}$ by which the predicted density $p(\mathbf{x}_k^r|\mathcal{Z}^{k-1})$ in road coordinates can be transformed into ground coordinates:

$$\underbrace{p(\mathbf{x}_k^r|\mathcal{Z}^{k-1})}_{\text{in road coordinates}} \xrightarrow[\text{road map errors}]{\text{road network}} \underbrace{p(\mathbf{x}_k^g|\mathcal{Z}^{k-1})}_{\text{in ground coordinates}}. \tag{29}$$

When available in ground coordinates, the linearized versions of the transforms from ground coordinates to sensor coordinates and vice versa, $\mathbf{t}_{s\leftarrow g}$ and $\mathbf{t}_{g\leftarrow s}$, can be used to represent the densities in sensor coordinates, where the filtering step is to be performed. To this end, we write the density $p(\mathbf{x}_k^g|\mathcal{Z}^{k-1})$ as a sum over the n_r road segments considered:

$$p(\mathbf{x}_k^g|\mathcal{Z}^{k-1}) = \sum_{m=1}^{n_r-1} p(\mathbf{x}_k^g|m, \mathcal{Z}^{k-1})\, p(m|\mathcal{Z}^{k-1}). \tag{30}$$

In equation 30 $p(m|\mathcal{Z}^{k-1})$ denotes the probability that the target moves on the segment m given the accumulated sensor data $\mathcal{Z}^{k-1}$ and is calculated in reference (3, 8). According to these references $p(\mathbf{x}_k^g|m, \mathcal{Z}^{k-1})$ can be calculated from the probability density in road coordinates and is approximately given by a Gaussian.

The inverse transform is simply provided by individually projecting the densities $p(\mathbf{x}_k^g|m, \mathcal{Z}^k)$ on the road (i.e. after the filtering step). Before the subsequent prediction is performed, it seems to be reasonable to apply a second-order approximation to the mixture densities:

$$p(\mathbf{x}_k^r|\mathcal{Z}^k) = \sum_{m=0}^{n_r} p(m|\mathcal{Z}^k)\, p(\mathbf{x}_k^r|m, \mathcal{Z}^k) \tag{31}$$

$$\approx \mathcal{N}\big(\mathbf{x}_k^r;\, \mathbf{x}_{k|k}^r,\, \mathbf{P}_{k|k}^r\big). \tag{32}$$

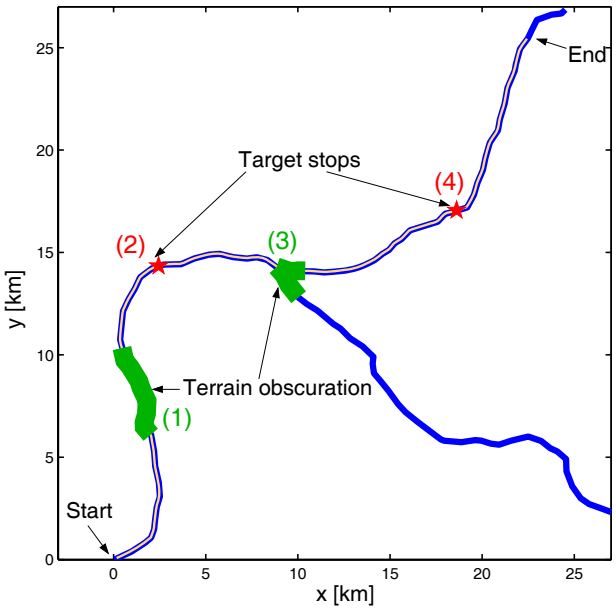

Figure 3: A GMTI tracking scenario.

6 DISCUSSION OF AN EXAMPLE

We discuss an example illustrating the iterative process of tracking-driven road map extraction sketched above.

6.1 A Simplified Scenario

Figure 3 shows a simulated and idealized, but non-trivial GMTI tracking scenario. On a road network a single ground vehicle is moving from 'Start' to 'End'. On its way it passes two regions, where it is not detectable by the radar sensor due to terrain obscurations. The second obscuration hides an intersection. The vehicle stops twice for several minutes (stars). Obviously, during these periods the vehicle is not detectable by a GMTI radar.

Directly before and after the second terrain obscuration the detection probability of the radar is significantly reduced due to the phenomenon of 'Doppler blindness'. In such regions the radial velocity of the moving vehicle relative to the moving sensor platform is equal or close to the corresponding radial velocity of the ground patch surrounding the vehicle. For this reason the skin echo of the vehicle can in most cases no longer be discriminated from the ground clutter returns by using Pulse-Doppler signal processing (STAP: Space Time Adaptive Processing (15)). The vehicle is thus masked by the 'clutter notch' of the GMTI radar.

The revisit interval of the simulated GMTI radar is 12 s. It is located in a distance of 100 km along the y-axis (stand-off radar). Its measurement accuracy (standard deviation) is 20 m in range (i.e.. along the y-axis) and 400 m in cross-range (i.e. along the x-axis). The corresponding Minimum Detectable Velocity (MDV) is 2 m/s. In this simplified example we exclude the treatment of false or unwanted radar returns and consider well-separated ground moving vehicles only. The total observation time is one hour (300 scans).

6.2 Simulation Results

Figure 4 shows the major and minor semi-axes of the error ellipses related to the position estimates of the vehicle as a function of the tracking time (solid and dashed lines, respectively). These

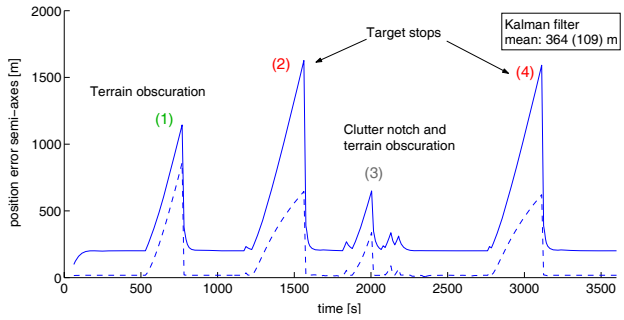

Figure 4: Filtering covariances (major/minor eigenvalues).

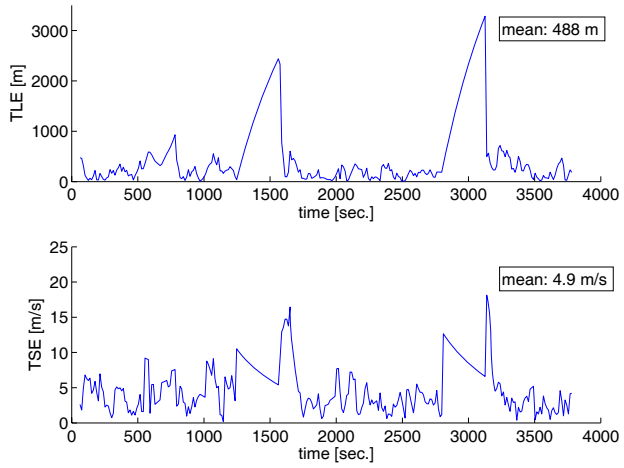

Figure 5: Tracking error (localization, speed).

quantities are simply obtained by applying Kalman filtering for tracking as there are no false returns or other vehicles in the vicinity. We observe four pronounced peaks which correspond the terrain obscurations, the vehicle stops, and the regions where the radar is Doppler-blind. The mean values of the semi-axes are 364 m and 109 m, respectively.

In figure 5 the tracking error, i.e. the distance between the simulated true vehicle state and the corresponding estimates, are displayed for a single run as a function of the tracking time (TLE: Target Localization Error, TSE: Target Speed Error). The corresponding mean values are 498 m and 4.9 m/sec, respectively. In the temporal evolution of the localization error only two peaks are visible. The orientation of the road is by chance along the resulting predictions in the situations where the other peaks occurred in the previous figure.

Figure 6 shows the major and minor semi-axes of the error ellipses of the retrodicted position estimates of the vehicle as a function of the tracking time (solid and dashed lines, respec-

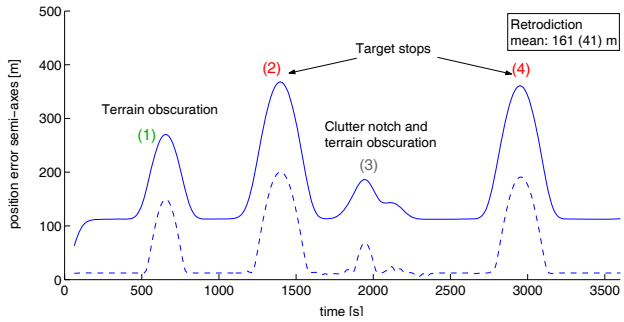

Figure 6: Retrodiction covariances (major/minor eigenvalues)

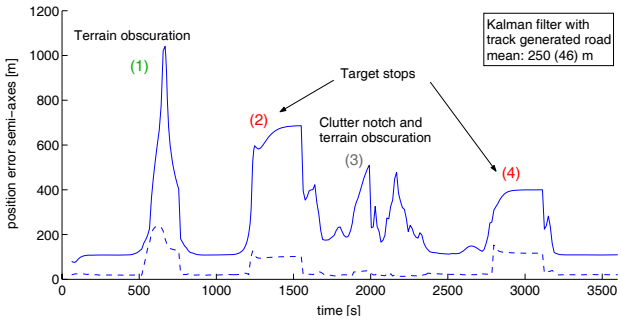

Figure 7: Filtering covariances (major/minor eigenvalues)

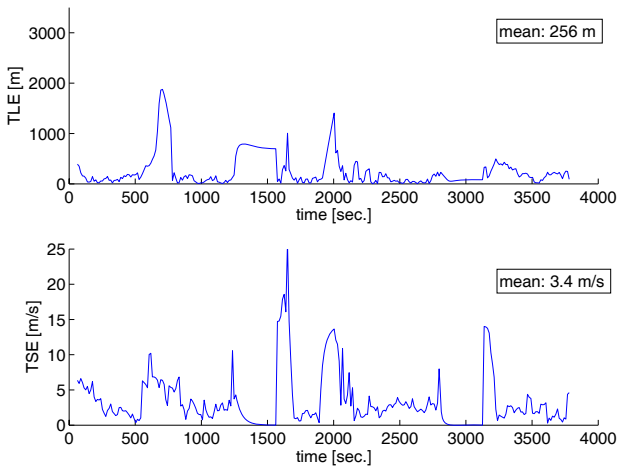

Figure 8: Tracking error (localization, speed)

tively). Obviously the error covariance matrices are much reduced in size (mean values 161 m and 41 m, respectively) and are used for describing the road map errors as discussed in the previous sections. The retrodicted state estimates of the road-moving vehicle are used for approximating the road.

This first approximation of the road map, which was reconstructed by the track of a first road moving vehicle, is now used for 'road map assisted tracking' of a second vehicle using the same road. In Figure 7 the resulting major and minor semi-axes of position error ellipses are shown. The mean values are 260 m and 46 m, respectively. Evidently, these quantities are much smaller than the corresponding quantities obtained in the previous case. In particular, the pronounced peaks in the time periods when the target stops are significantly smaller. The same tendencies can be observed in Figure 8, which shows the tracking errors for localization and speed (mean values: 256 m and 3.4 m/sec, respectively). As expected, by road map information only a slight improvement in the velocity estimates is obtained.

The next step for improving the underlying road map to be extracted consists in applying retrodiction to this track being more accurate than the track used in the first step of the iteration.

In Table 1 the mean values of the accuracies previously discussed are summarized. P and p denote the major and minor eigenvalues of the corresponding covariance matrices. Even by this first iteration for reconstructing a road map from GMTI tracks an error reduction in position of about 30 – 50% can be obtained if this road is used for road map assisted tracking. We expect that by iterating this procedure under different sensor-to-target geometries and with a more refined continuous time retrodiction technique, such as described in section 4, highly accurate roads can finally be obtained.

tracker	P [m]	p [m]	TLE [m]	TSE [m/s]
no road	364	109	489	4.9
road	250	46	256	3.4

Table 1: Relevant accuracies (mean values).

7 CONCLUSIONS

We discussed ground moving vehicle tracking as a means for extracting road map information from GMTI radar data. The resulting tracking-generated road maps are highly up-to-date. By iteratively applying the described procedures, the produced maps can be highly precise as well. Moreover, their accuracy in each node is quantitatively described. The proposed approach to road map extraction is essentially based on a temporal integration of the received sensor data and by this differs in nature from methods based on pattern recognition in a single image.

We summarize some aspects, which might be of particular interest in view of sensing applications:

- Tracking-driven road extraction can be beneficial in situations or scenarios where reliable road maps are not or not yet available, where the road maps provided by geographical information systems are not up-to-date, or where the accuracy of existing road maps is insufficient.
- In certain applications roads or road-like 'lines of communication' exist only temporarily or may change with time. As practical evidence shows, even in typical off-road scenarios structures similar to roads quickly evolve, as a 'second' vehicle usually moves in the 'tracks' of its precursor.
- As usually many targets use the same road, a significant gain results from fusing several 'road tracks'. For airborne GMTI radar the sensor-to-target geometry is continuously changing. Therefore the fusion 'road tracks' produced at different times improves the achievable accuracy even more.
- Sensor registration or misalignment errors usually cause serious problems in multiple sensor data fusion. For mitigating these phenomena, precisely extracted road maps can be matched with each other, thus compensating relative bias errors. For removing absolute bias errors, matching with geo-referenced road maps can be used.

REFERENCES

KIRUBARAJAN, T., BAR-SHALOM, Y., PATTIPATI, K.R., KADAR, I., 'Large Scale Ground Target Tracking With Single and Multiple MTI Sensors', Chapter 6 in: Y. Bar-Shalom, Blair, W.D. (Eds.), *Multitarget-Multisensor Tracking Applications and Advances III*, Boston, MA: Artech House, 2000.

KOCH, W., KLEMM, R., 'Ground Target Tracking with STAP Radar', *IEE Proceedings Radar, Sonar and Navigation Systems*, Special Issue: Modeling and Simulation of Radar Systems, 2001, Vol. 148, No. 3, invited paper.

KOCH, W., 'GMTI-Tracking and Information Fusion for Ground Surveillance', *Signal and Data Processing of Small Targets*, **SPIE Vol. 4473**, pp.381-393, San Diego, USA, August 2001.

KOCH, W., Ground Target Tracking with STAP Radar: Selected Tracking Aspects. Chapter 15 in: R. KLEMM (Ed.), *The Applications of Space-Time Adaptive Processing*, IEE Publishers (2004).

P. J. Shea, T. Zadra, D. Klamer, E. Frangione, and R. Brouillard, "Improved state estimation through use of roads in ground tracking," in *Proc. of Signal and Data Processing of Small Targets*, O. E. Drummond, Ed., vol. 4048, SPIE, 2000, pp. 321–332.

C. Agate and K. J. Sullivan, "Road-constraint target tracking and identification using a particle filter," in *Proc. of Signal and Data Processing of Small Targets*, O. E. Drummond, Ed., vol. 5204, SPIE, 2003.

M. S. Arulampalam, N. Gordon, M. Orton, and B. Ristic, "A variable structure multiple model particle filter for GMTI tracking," in *Proc. Int. Conf. Information Fusion*. Annapolis: ISIF, July 2002, pp. 927–934.

ULMKE, M., 'Improved GMTI-Tracking using Road-Maps and Topographical Information', Proceedings of: *SPIE Signal and Data Processing of Small Targets 2003*, Vol. 5204, July 2003.

ULMKE, M., KOCH, W., 'On Road-Map Assisted GMTI Tracking', Proceedings of: *DGON German Radar Symposium GRS'02*, pp. 89-93, Bonn, Germany, September 2002.

BAR-SHALOM, Y., LI, X.-R., AND KIRUBARAJAN, T., *Estimation with Applications to Tracking and Navigation*, Wiley & Sons, 2001.

BLACKMAN, S., POPULI, R., *Design and Analysis of Modern Tracking Systems*, Artech House, 1999.

KOCH, W., Target Tracking. Chapter 8 in: S. Stergiopoulos (Ed.), *Advanced Signal Processing Handbook: Theory and Applications for Radar, Sonar, and Medical Imaging Systems*, CRC Press, 2000.

KOCH, W., 'Fixed-Interval Retrodiction Approach to Bayesian IMM-MHT for Maneuvering Multiple Targets', *IEEE Transactions on Aerospace and Electronic Systems*, **AES-36**, 1 (2000)

VAN KEUK, G., BLACKMAN, S., 'On Phased-Array Tracking and Parameter Control', *IEEE AES **29***, No. 1 (1993).

KLEMM, R., 'Principles of space-time adaptive processing', London, UK, *IEE Publishers*, 2002.